

Two-photon excitation spectroscopy of coupled asymmetric GaN/AlGaN quantum discs

K H Lee¹, S Birner², J H Na¹, R A Taylor¹, S N Yi^{1,3}, Y S Park⁴,
C M Park⁴ and T W Kang⁴

¹ Department of Physics, University of Oxford, Parks Road, Oxford OX1 3PU, UK

² Walter Schottky Institute and Physics Department, Technical University of Munich, D-85748 Garching, Germany

³ Department of Semiconductor Physics, Korea Maritime University, Busan 606-791, Korea

⁴ Quantum-functional Semiconductor Research Centre, Dongguk University, Seoul 100-715, Korea

E-mail: rtaylor1@physics.ox.ac.uk

Received 14 September 2006, in final form 15 October 2006

Published 10 November 2006

Online at stacks.iop.org/Nano/17/5754

Abstract

By using two-photon excitation spectroscopy we take advantage of the increased spatial resolution to perform time-integrated and time-resolved photoluminescence measurements on several discrete stacks of GaN quantum discs. The stack structure consisted of coupled asymmetric GaN quantum discs with embedded AlGaN barriers, which were grown at the tip of a GaN nanocolumn. We observed that with increasing optical excitation power the carrier lifetime decreased due to free-carrier screening, with an enhancement of the screening effect in the larger quantum disc due to carrier tunnelling from the smaller quantum disc.

1. Introduction

Two-photon excitation (TPE) spectroscopy is a powerful method of investigating the properties of nanostructures. It has been used to directly excite and study the properties of higher order 2p excitonic states in GaAs/AlGaAs quantum wires [1], analyse spatial distribution of defects in InGaN light emitting diodes [2] and map the piezoelectric field distribution in bulk GaN and InGaN multiple quantum wells (MQWs) [3]. TPE relies on the nonlinear absorption of high peak power laser pulses at a wavelength that is too long to excite by single-photon excitation (SPE). Due to the nonlinearity, TPE spectroscopy has several advantages compared to conventional SPE spectroscopy. The quadratic intensity dependence of TPE enhances the spatial resolution, allowing sub-diffraction limit resolution to be achieved. As the excitation is more localized and not all materials luminesce when excited by a wavelength smaller than the bandgap, improved background discrimination can also be achieved.

In this paper we use TPE spectroscopy to investigate the optical properties of discrete coupled asymmetric GaN quantum discs (Q-discs) with embedded AlGaN barriers. We

define a Q-disc as a QW like structure grown at the tip of a GaN nanocolumn, while a Q-disc *stack* is a complete MQW like structure, also at the tip of a nanocolumn (figure 1). We employ time-resolved (TR-) and time-integrated (TI-) photoluminescence (PL) measurements and multi-band $\mathbf{k} \cdot \mathbf{p}$ computational modelling to investigate the Q-discs. There were two broad motivations for this study. First, III nitride nanostructures have attracted much attention due to their application in blue/ultra-violet wavelength optoelectronic devices with enhanced device performance, i.e. higher quantum efficiency and improved optical gain. Furthermore, self-organized GaN nanocolumns possess desirable properties such as low defect density, good geometry and alloy composition reproducibility, and they can be grown monolithically by molecular beam epitaxy (MBE). This makes nanocolumns an attractive basis for novel, optically active devices. Significant advancements have been made towards practical devices, with GaN nanocolumns incorporating Bragg reflectors being fabricated [4] and stimulated emission being demonstrated [5]. Secondly, TPE spectroscopy involving III nitride materials has been limited to either bulk [6] or QWs [2, 8], but not nanocolumns—which is

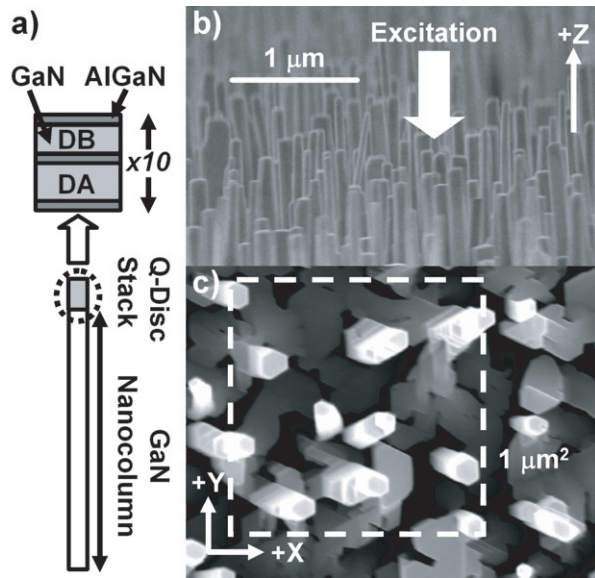


Figure 1. (a) Illustration of the GaN Q-discs stack structure. The GaN Q-discs are embedded at the top region of the nanocolumn. (b) Cross-sectional and (c) top view SEM images of the sample, showing the hexagonal columnar structure and the orientation of the excitation.

more challenging due to the geometry. Our motivation was to utilize TPE to investigate the optical properties of discrete Q-disc stacks and compare this with previous SPE studies [7, 9]. Interesting behaviour such as free-carrier screening has been previously observed and this could have an important effect on the device characteristics, such as emission wavelength and carrier dynamics.

2. Experimental details

The GaN/AlGaIn Q-discs were grown at the tip of a $2.7 \mu\text{m}$ high GaN nanocolumn, with the GaN nanocolumn and Q-disc grown using plasma assisted MBE on a Si(111) substrate without any buffer layer [10] (figures 1(a), (b)). As illustrated in figure 1(a) the Q-disc stack consisted of ten periods of two alternating GaN Q-disc thicknesses (4 and 3 nm) separated by an $\text{Al}_{0.5}\text{Ga}_{0.5}\text{N}$ barrier with an effective thickness of ~ 1 nm. In this paper the larger Q-disc is referred to as DA, while the smaller Q-disc is referred to as DB. Modelling this structure by *nextnano*³, a multi-band $\mathbf{k}\cdot\mathbf{p}$ nanostructure simulator [11], DA and DB peak emissions were calculated to be 3.45 and 3.55 eV, respectively. As seen in the electron micrograph in figure 1(c) the GaN nanocolumns exhibited a density of $1 \times 10^9 \text{ cm}^{-2}$ and an average diameter of 100 nm—hence demonstrating lateral confinement. From our previous studies the emission from GaN nanocolumns was observed at 3.58 eV—the blue-shift arising from reduced dimensionality and confinement effects [7, 12].

The Q-disc sample was characterized using a combination of TI- and TR-PL measurements. As illustrated in figure 1(b), the sample was excited under vertical orientation and the carriers were strongly confined to the Q-disc region. The optical configuration for TPE spectroscopy was identical to that employed for SPE spectroscopy (hence allowing

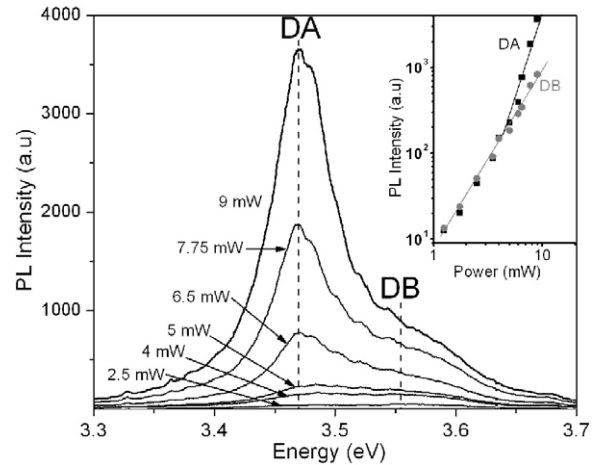


Figure 2. TI-PL spectra of the GaN Q-discs under TPE excitation. Inset shows a plot of peak intensity versus excitation power.

comparisons to be made), with the only noticeable change being the excitation source. For TPE spectroscopy excitation was provided by a frequency-doubled femtosecond Ti:sapphire laser pulses at 430 nm (pulse width of 120 fs and a repetition frequency of 76 MHz). This corresponded to an excitation energy of 2.88 eV (below GaN bandgap of ~ 3.55 eV), but under TPE conditions, this equated to an excitation of 5.76 eV (above GaN bandgap). Hence, the Q-discs were excited well above the bandgap, under nonresonant conditions.

The sample was mounted in a continuous-flow helium cryostat (Janis ST-500) with the temperature maintained at 4 K. A $36\times$ reflecting objective (Ealing) was mounted on a piezo-stage (Melles Griot Nano-Max) and held above the cryostat to both focus the incident laser beam to a spot size of $\sim 2 \mu\text{m}$ and to collect the resulting luminescence. The PL was dispersed by a 0.3 m spectrograph, which was equipped with a $1200 \text{ grooves mm}^{-1}$ grating. For TI measurements the PL was detected by a Peltier-cooled CCD, and for TR measurements the PL was directed to a commercial time-correlated single-photon counting system using a photomultiplier tube (PMT) as a detector (120 ps resolution).

3. Experimental results

3.1. TI-PL measurements

TPE spectra as a function of excitation power ranging from 2.5 to 9 mW (at the focus) are presented in figure 2. Two peaks were observed at 3.48 and 3.56 eV, labelled DA and DB in the spectra. This was in good agreement with the calculated values using *nextnano*³. We ensured that only a few Q-disc stacks were excited by maximizing the intensity of the DA peak through precise movements of the piezo-stage. Further discussions of the spatial dependence is presented in section 3.2. The inset in figure 2 shows the relationship between the peak intensity and excitation power. The DB peak intensity I_{DB} displayed a quadratic (slope = 2) dependence with excitation power (i.e. equivalent of linear PL dependence under SPE conditions), while DA peak intensity I_{DA} displayed a higher order dependence (slope > 2) with excitation power.

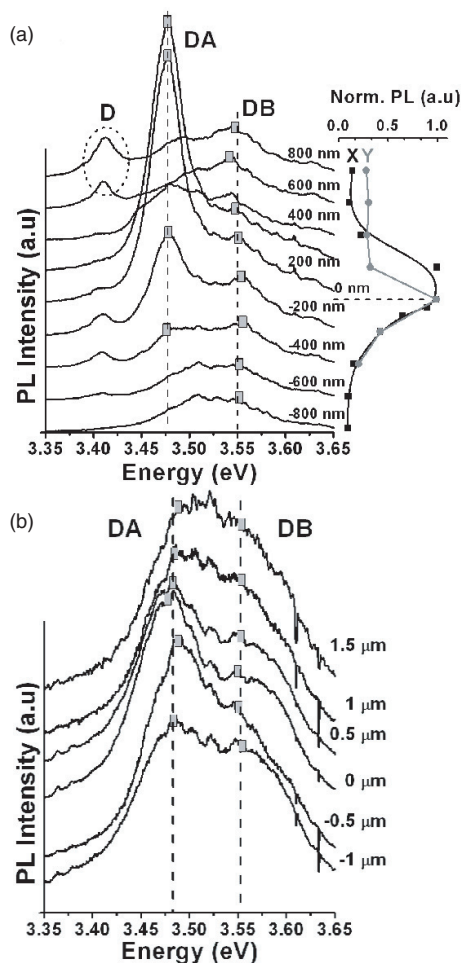


Figure 3. (a) Series of TI-PL spectra taken 200 nm apart (in X direction) to demonstrate the increased spatial resolution of TPE spectroscopy. Plot on the right show the profile of DA peak intensity variation along X and Y direction. (b) Series of TI-PL spectra taken 500 nm apart using SPE excitation.

This was clearly evident for excitation powers greater than 4 mW. Nonlinear PL dependence with excitation power, due to carrier tunnelling, has been observed in earlier SPE studies involving GaAs/AlGaAs asymmetric QWs [13].

3.2. Improved spatial resolution

We illustrate the increased spatial resolution offered by TPE spectroscopy by demonstrating that only a few discrete Q-disc stacks were excited by the beam. We excited the sample at 9 mW and observed the resulting TI-PL spectrum as the beam was moved laterally over the sample using the piezo-stage (figure 3(a)). The orientation for the lateral movement corresponded to the axis labelled in figure 1(c).

The TPE data show that only one or two Q-disc stacks were excited. Firstly, over the region of interest I_{DA} rapidly decreased for $\sim\pm 200$ nm radial movements from the peak. This is supported by the fact that the nanocolumns (and consequently the Q-disc stacks which are grown at the tip) have an average diameter of ~ 100 nm and an average density of $\sim 10 \mu\text{m}^{-2}$. For comparison, the spatially dependent TI-PL

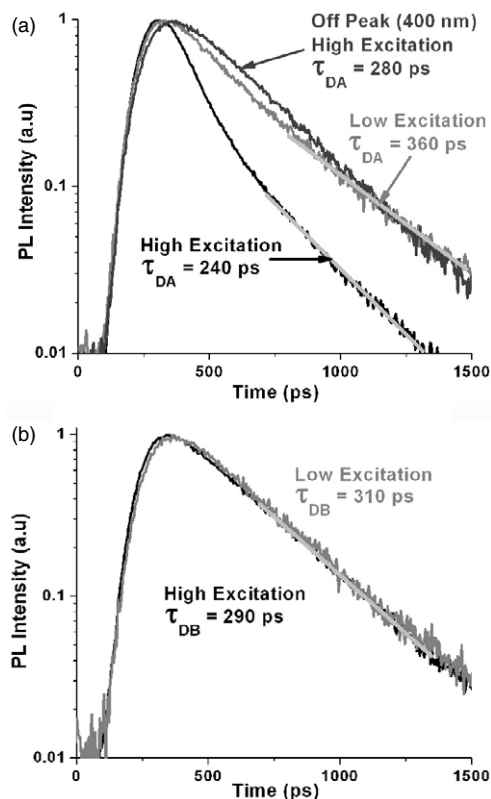


Figure 4. TR-PL measurement from DA (a) and DB (b), at low and high excitation powers.

spectra obtained under SPE conditions (266 nm or 4.65 eV) is presented in figure 3(b). It can be observed that even with $\pm 1 \mu\text{m}$ movements the PL spectra did not change significantly ($\sim 20\%$). The 266 nm beam was strongly absorbed over the $\sim 2 \mu\text{m}$ beam spot size, leading to an ensemble response, while under TPE conditions the beam was highly localized. Secondly, the sensitivity of the tunnelling is illustrated in figure 3(a). Radial movements of ± 200 nm from the peak lead to a rapid decrease in the I_{DA} and when the beam was ± 400 nm from the peak the DA and DB peak intensities became comparable. Under these conditions the Q-disc stack was weakly excited, leading to reduced tunnelling and emission originating from the carriers generated within the respective Q-discs. It was not possible to observe this behaviour under SPE conditions, since we could only achieve an ensemble response. Lastly, the peak at ~ 3.41 eV (labelled 'D' on figure 3(a)) originated from extended structural defects located at the nanocolumn–substrate interface [14, 15]. Subsequent investigation with TR-PL showed that the carrier lifetime was ~ 1 ns for this peak.

3.3. TR-PL measurements

By using the increased spatial resolution offered by TPE spectroscopy we performed TR-PL measurements on several discrete Q-disc stacks to study the carrier lifetimes. For the TR-PL measurements the beam was re-positioned at the peak of the TI-PL response in figure 3(a). Figures 4(a) and (b) show the TR-PL trace collected from the DA and DB peaks, at high

(9 mW) and low (2.5 mW) excitation powers. The TR-PL traces show a mono-exponential decay at low excitation power, with fitted lifetimes of $\tau_{DA} = 360$ ps for DA and $\tau_{DB} = 310$ ps for DB. At high excitation power the lifetimes decreased to $\tau_{DA,HI} = 240$ ps and $\tau_{DB,HI} = 290$ ps. In addition, the DA trace showed a bi-exponential decay with a fast component of $\tau_1 = 140$ ps. The fast component was identified with free-carrier decay, which had a more significant contribution with increasing optical excitation. Since the carrier density decreases due to recombination, the PL decay time becomes longer over time, resulting in bi-exponential decay. The bi-exponential decay is also present in DB but occurs on a shorter time scale than in DA and the effect is weaker [9]. Hence, given the lower resolution of the PMT, it was not possible to observe this directly in our measurements.

4. Discussion

The TI-PL and TR-PL results show evidence of free-carrier screening and this is consistent with the results from the earlier studies performed under SPE [9]. The decrease in τ_{DA} and τ_{DB} with increasing optical excitation is caused by photo-generated free carriers screening the built-in piezoelectric and pyroelectric fields [16, 17], which are responsible for the quantum confined Stark effect (resulting in a red-shift and spatial separation of the electrons and holes). This then leads to an increased overlap between the electrons and holes, which corresponds to an increased oscillator strength (stronger peak intensity and decreased carrier lifetime). Therefore the nonlinear PL response and reduction of carrier lifetime, with increasing excitation power arises from the same mechanism. However this effect is significantly enhanced in DA due to the carriers tunnelling from DB to DA, which provides additional free carriers, and hence further screening the built-in fields. Investigation with nextnano³ predicted the tunnelling of carriers from DB to DA. For example, the ground state electron in DB can tunnel through the AlGa_{0.2}N barrier and extend into DA. However, the converse was not true as the electron was strongly localized in DA [9]. (For simplicity we have considered the electron behaviour, but a similar behaviour must be present for holes; otherwise we would have a growing excess number of holes.)

Furthermore, the increased spatial resolution provided by TPE allowed observation of several interesting results, otherwise not possible under SPE. Firstly, further evidence of free-carrier screening enhancement was observed. While under high excitation power, the beam was moved away from the Q-disc stack by 400 nm (along the XY plane). As seen in figure 3(a), this corresponded to the condition when the DA and DB peak intensities were approximately equal $I_{DA}/I_{DB} \sim 1$. As a result $\tau_{DA,HI}$ increased from 240 to 280 ps, TR-PL response became mono-exponential and the photon count dropped to 5% of the peak value (figure 4(a)). Moving the beam away from the peak resulted in the Q-disc stack being weakly excited, leading to a reduction in the tunnelling. Thus the PL emission originated mainly from the carriers generated within the respective Q-discs. Hence, TPE allows the measurement of the ‘natural’ carrier lifetime, *without* the effect of enhancement due to tunnelling. Such measurements were not possible under SPE spectroscopy, as discrete Q-disc stacks could not be resolved for selective excitation.

Secondly, the higher excitation powers and more energetic carriers in TPE resulted in a subtle difference in the variation of τ_{DA} with increasing excitation powers, when compared to SPE. As discussed, decrease in carrier lifetimes with increasing optical excitation arises from free-carrier screening, and there is further enhancement of the free-carrier screening in DA due to the carrier tunnelling. Furthermore, under TPE it was observed that $\tau_{DA,HI} < \tau_{DB,HI}$, while $\tau_{DA,HI} \simeq \tau_{DB,HI}$ for SPE. We believe that this effect ($\tau_{DA,HI} < \tau_{DB,HI}$) in TPE arises from several mechanisms. TPE involves significantly larger excitation powers (an order of magnitude higher) and a more strongly localized beam (nonlinearity). Hence, combined with the high spatial resolution, it is possible to apply an intense beam at a discrete Q-disc stack and generate significant number of free carriers, which could contribute towards the free-carrier screening. This view is supported by the observation that at high excitation powers $I_{DA}/I_{DB} \sim 4$ under TPE while $I_{DA}/I_{DB} \sim 1.5$ under SPE [9]. Furthermore, the TPE condition used in this study involved injection of more energetic carriers (5.76 eV, as opposed to 4.65 eV in SPE), hence allowing for greater enhancement of the free-carrier screening effect, and greater relaxation time required for electron–hole recombination. This could help to explain why smaller $\tau_{DA,HI}$ could be obtained using TPE (240 ps) than through SPE (300 ps).

Lastly, the carrier lifetime behaviour demonstrates the low defect density of the GaN Q-discs (which is consistent with the properties of a self-assembled structure). For example, TR-PL measurements of a free-standing GaN film by Zhong *et al* demonstrated that the carrier lifetimes under SPE and TPE differed by an order of magnitude [9]. The short carrier lifetimes obtained using SPE was attributed to surface defects—which could act as nonradiative recombination centres. In comparison, carrier lifetimes in our GaN Q-discs were similar under SPE and TPE—which demonstrates that even under SPE, when a larger volume of the sample is excited, there is minimal interaction with surface defects.

5. Conclusion

In summary, the optical properties of several discrete GaN Q-disc stacks were investigated using TPE spectroscopy. Consistent with SPE measurements, we observed evidence of free-carrier screening (nonlinear PL response and reduction of carrier lifetime, with increasing excitation power), with an enhancement of the screening due to carrier tunnelling from DB to DA. By taking advantage of the improved spatial resolution offered by TPE, it was possible to measure the carrier lifetimes in the presence and absence of the enhancement effect, due to the carrier tunnelling. Furthermore, by comparing carrier lifetimes obtained using SPE and TPE, the low defect nature of the self-assembled GaN Q-disc was demonstrated.

Acknowledgments

This research is part of the QIP IRC supported by EPSRC (GR/S82176/01). KHL thanks the University College old members fund scholarship, Clarendon Fund bursary, Overseas Research Students award, and M A G Jones for computational support. YSP is grateful for the support of the Korea

Research Foundation Grant funded by the Korean government (MOEHRD, Basic Research Promotion Fund) (KRF-2006-312-C00162) and QSRC at Dongguk University.

References

- [1] Cingolani R, Lepore M, Tommasi R, Catalano I M, Lage H, Heitmann D, Ploog K, Shimizu A, Sakaki H and Ogawa T 1992 *Phys. Rev. Lett.* **69** 1276
- [2] Kao F-J, Huang M-K, Wang Y-S, Huang S-L, Lee M-K and Sun C-K 1999 *Opt. Lett.* **24** 1407
- [3] Sun C-K, Chu S-W, Tai S-P, Keller S, Abare A, Mishra U K and DenBaars S P 2001 *Scanning* **23** 182
- [4] Ristić J, Calleja E, Trampert A, Fernández-Garrido S, Rivera C, Jahn U and Ploog K H 2005 *Phys. Rev. Lett.* **94** 146102
- [5] Kikuchi A, Yamano K, Tada M and Kishino K 2004 *Phys. Status Solidi b* **241** 2754
- [6] Kim D, Libon I H, Voelkmann C, Shen Y R and Petrova-Koch V 1997 *Phys. Rev. B* **55** R4907
- [7] Na J H, Taylor R A, Rice J H, Robinson J W, Lee K H, Park Y S, Park C M and Kang T W 2005 *Appl. Phys. Lett.* **86** 083109
- [8] Zhong Y, Wong K S, Zhang W and Look D C 2006 *Appl. Phys. Lett.* **89** 022108
- [9] Lee K H, Na J H, Taylor R A, Yi S N, Birner S, Park Y S, Park C M and Kang T W 2006 *Appl. Phys. Lett.* **89** 023103
- [10] Park C M, Park Y S, Hyunsik I and Kang T W 2006 *Nanotechnology* **17** 952
- [11] nextnano³ device simulator: The program is available at www.wsi.tum.de/nextnano3 and www.nextnano.de
- [12] Na J H, Taylor R A, Rice J H, Robinson J W, Lee K H, Park Y S, Park C M and Kang T W 2005 *Appl. Phys. Lett.* **86** 123102
- [13] Leopold D J and Leopold M M 1990 *Phys. Rev. B* **42** 11147
- [14] Ristić J, Calleja E, Sánchez-García M A, Ulloa J M, Sánchez-Páramo J, Calleja J M, Jahn U, Trampert A and Ploog K H 2003 *Phys. Rev. B* **68** 125305
- [15] Park Y S, Lee S-H, Oh J-E, Park C-M and Kang T-W 2005 *J. Cryst. Growth* **282** 313
- [16] Sala F D, Di Carlo A, Lugli P, Bernardini F, Fiorentini V, Scholz R and Jancu J-M 1999 *Appl. Phys. Lett.* **74** 2002
- [17] Kuroda T, Tackeuchi A and Sota T 2000 *Appl. Phys. Lett.* **76** 3753